Med Biol Eng Comput (2011) 49:593–604
DOI 10.1007/s11517-011-0761-z

SPECIAL ISSUE - ORIGINAL ARTICLE

A novel method for recording neuronal depolarization with recording at 125–825 Hz: implications for imaging fast neural activity in the brain with electrical impedance tomography

T. Oh · O. Gilad · A. Ghosh · M. Schuettler · D. S. Holder

Received: 12 December 2010 / Accepted: 10 March 2011 / Published online: 30 March 2011

Abstract Electrical impedance tomography (EIT) is a recently developed medical imaging method which has the potential to produce images of fast neuronal depolarization in the brain. Previous modelling suggested that applied current needed to be below 100 Hz but the signal-to-noise ratio (SNR) recorded with scalp electrodes during evoked responses was too low to permit imaging. A novel method in which contemporaneous evoked potentials are subtracted is presented with current applied at 225 Hz to cerebral cortex during evoked activity; although the signal is smaller than at DC by about 10×, the principal noise from the EEG is reduced by about 1000×, resulting in an improved SNR. It was validated with recording of compound action potentials in crab walking leg nerve where peak changes of −0.2% at 125 and 175 Hz tallied with biophysical modelling. In recording from rat cerebral cortex during somatosensory evoked responses, peak impedance decreases of $-0.07 \pm 0.006\%$ (mean ± SE) with a SNR of >50 could be recorded at 225 Hz. This method provides a reproducible and artefact free means for recording resistance changes during neuronal activity which could form the basis for imaging fast neural activity in the brain.

Keywords Neurophysiology · Impedance · Electrical impedance tomography · Nerve · Compound action potential · Crab · Rat · Cortical evoked responses

T. Oh · O. Gilad · A. Ghosh · D. S. Holder (✉)
Department of Medical Physics, University College London, London, UK
e-mail: d.holder@ucl.ac.uk

T. Oh
Bio-Medical Engineering Dept, Kyunghee University, Yongin, South Korea

O. Gilad
Corotix Technologies Ltd., 29 Inbar St, 30900 Zichron Yaakov, Israel

A. Ghosh
Department of Neurosurgery, King's College Hospital, London, UK

M. Schuettler
Department of Microsystems Engineering, IMTEK University of Freiburg, Freiburg, Germany

1 Introduction

Functional neuroimaging has improved greatly in the past two decades but the 'holy grail' would be to image fast neuronal activity non-invasively with a time and spatial resolution of about 1 ms and 1 mm, respectively. Electrical impedance tomography (EIT) is a novel medical imaging method which has the potential to achieve this major advance, by imaging changes in electrical impedance over milliseconds [22] which occur when neuronal ion channels open during activity and the cell membrane resistivity decreases [8]. The underlying purpose of this work was to develop a method which could form the basis for tomographic imaging of resistance changes during neuronal depolarization in the brain. EIT provides information regarding the internal electrical properties inside a body based on non-invasive voltage measurements on its boundary. Data acquisition is performed through an array of electrodes which are attached to the boundary of the imaged object. Sequences of small insensible currents, typically about of 1 mA, are injected into the object through these electrodes and the corresponding boundary electric potentials are measured over a predefined set of

electrodes. The process is repeated for numerous different configurations of applied current. The internal admittivity (or impedivity) distribution can be inferred using this boundary data. EIT was initially applied to chest imaging [5, 34]. Potential applications of EIT for imaging brain function and pathology include detection and monitoring of cerebral ischaemia and haemorrhage [24, 33, 38], localisation of epileptic foci [10], normal haemodynamic brain function [41] and fast neuronal activity [4, 22].

The principle by which EIT could image neuronal activity rests on the application of low frequency currents below about 100 Hz which remain in the extracellular space under resting conditions because they cannot enter significantly into the intracellular space across the capacitative cell membrane. During the action potential or neuronal depolarization, the membrane resistance diminishes by about 80× [8] so that the applied current enters the intracellular space as well. Over a population of neurones, this will lead to a net decrease in the resistance during coherent neuronal activity, such as cortical evoked responses, as the intracellular space will provide additional conductive ions. The magnitude of such fast changes in the brain has been investigated by modelling and animal studies in our group. With biophysical modelling based on cable theory, the local resistivity changes with recording near DC were estimated to be 2.8–3.7% for peripheral nerve bundles and 0.06–1.7% for the cortex during evoked potentials (EP) [3, 32]. These predictions are in broad agreement with measured near DC decreases of 0.5–1.0% in crab peripheral nerve [3, 18, 25].

Based on this biophysical modelling, a method was developed for recording such fast neural activity, using a square wave injected constant current at about 1 Hz [16–19, 25]. The principle was to average following a repeated physiological stimulus, such as an alternating chequerboard or electrical stimulation of the median nerve at the wrist. A safe, insensible, constant current was injected over the relevant part of the brain and the resulting voltages were recorded from electrodes placed adjacently. The temporal resolution was only limited by the sampling speed and could in principle be less than 1 ms. This may be undertaken with epicortical electrodes placed on cerebral cortex, or scalp electrodes, in awake humans or experimental animals or, for purposes of validation, in peripheral nerve.

Unfortunately, the method is not straightforward. In principle, the signal should be a transient decrease in voltage lasting for about 30 ms on the background of a square wave produced by the injected current. This may be very small—an impedance decrease of 1% locally in the brain may reduce to 0.01% or smaller if recorded distantly on the scalp [19]. In addition, recording lies within the bandwidth of endogenous nervous activity—electroencephalogram (EEG), electrocorticogram (ECoG), EP or compound action potential—so that the voltages recorded from the injected square wave for impedance recording are mixed with the endogenous potentials. Uncorrelated signals, such as the EEG, may be reduced by averaging, whereas correlated ones, such as the evoked potentials, may be removed by subtraction. However, for this to be effective, the injected current for impedance measurement must not significantly alter the evoked potential, so this limits the current which may be injected. An effective method has been developed based on subtraction of paired recordings and control traces, with advanced signal processing to remove outliers and technical obstacles such as gradual decreases in applied voltage due to drift in batteries [16, 18].

A human study was undertaken during visual evoked responses and recording with either scalp electrodes or magnetoencephalography (MEG) with special cup electrodes filled with paste to minimise stimulation of cutaneous skin receptors on the scalp [17]. It was possible to record significant, reproducible, peak resistance decreases of $0.001 \pm 0.0005\%$ ($n = 16$ in 6 subjects) (mean ± SE) which supported the modelling, but, unfortunately, the SNR in individual subjects was too low to support EIT imaging in a practicable time. This was encouraging in that it supported the magnitude of local cortical changes estimated by biophysical modelling but disappointing with respect to human imaging [16]. Analysis of the human data indicated that the limiting factor was the uncorrelated EEG (or ECoG for cortical recording) rather than instrumentation noise. This was about two orders of magnitude greater than the resistance changes. It could be overcome by averaging, but the time needed to do this prevented practical imaging in a reasonable time in the human study above. The original modelling indicated that recording should be as near to DC as possible [3] (Fig. 1), in order to deliver the largest possible signal, but consideration of the above main noise source led to the unexpected conclusion that recording at a higher frequency of a few hundred Hz may produce a higher signal-to-noise ratio (SNR), as the power of the ECoG or EEG falls off more rapidly with frequency than the resistance change. For example, for epicortical recording, at 225 Hz, compared to at DC, the resistance change during depolarization falls by about 10× to 0.1% but the ECoG falls by 1000× to about 1 μV, so that the SNR increases by two orders of magnitude (Fig. 1).

The ultimate purpose of this work was to develop a method for recording resistance changes during neuronal depolarization in the brain, with the intention of using it to form EIT images of fast neural activity in the future. Such neural images might be with epicortical arrays or scalp electrodes, and in humans or animal studies. The advantage would be that images would be formed without the use of electrodes which penetrate into the substance of the brain and enable imaging of the entire cerebrum at once.

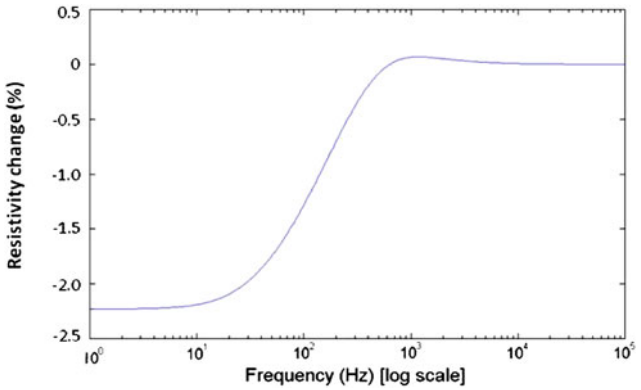

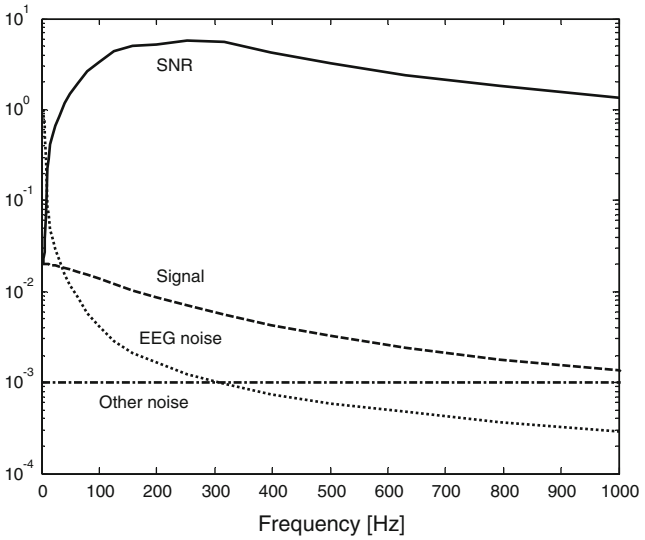

Fig. 1 *Left* Predicted resistivity change versus frequency (see Sect. 1) [3, 32]). *Right* Diagrammatic illustration of relative amplitudes of signal: resistance change during fast neural activity, EEG noise amplitude, and the resulting SNR over frequency. The signal and EEG noise are normalised and shown in arbitrary units. The EEG amplitude is the average of 28 channels recorded from rat cortex during anaesthesia with halothane (Sect. 2.3.2), resistance change is from biophysical modelling for cerebral cortex, and 'other noise' is instrumentation noise scaled to the EEG. It may be seen that the EEG decreases more rapidly over frequency than the resistance change, so that the SNR is maximal at c. 300 Hz

The purpose of this paper is to present this method (termed 'LF-EIT' (low frequency EIT)). It has been developed and refined using the compound action potential in crab peripheral nerve, in which the resistance change occurs contemporaneously with the compound action potential. Experimental results for this preparation are presented to demonstrate use of the method and provide evidence that the changes observed appear to be physiological and are not artefactual. The validated method was then assessed during evoked physiological activity in the cerebral cortex of the anaesthetized rat. Some examples of single channel data from these rat studies are presented here to illustrate the method in use.

2 Methods

2.1 Rationale of novel method for recording fast neural activity in the brain by EIT with applied sine wave at some hundreds of Hz

The principle of the new method is similar to that for square wave recording (Fig. 2). It is still necessary to employ signal processing and collection of pairs of data related to successive evoked stimuli, but the carrier is now a sine wave. Modelling suggested that the optimum was at about 300 Hz (Fig. 1); we have investigated currents applied from 125 to 825 Hz. As previously, nervous activity is evoked at about 2 Hz. A constant current sine wave is injected and is phase locked to the stimulus. The first of each pair of evoked stimuli is in phase and the second is in antiphase. The recorded voltage then comprises the voltages arising from (i) the sine wave carrier, (ii) its modulation by the impedance change, and (iii) the evoked nervous activity. Successive pairs of such stimuli and signals are averaged together—typically about 60 pairs over 1 min. The evoked nervous activity may then be obtained by summing the first and second segment, as the carrier signals are in antiphase and cancel. The impedance change was obtained by demodulating the result of subtracting the two segments, so that the evoked response cancelled out. On the basis that the phase angle of nervous tissue is less than 10° up to 1 kHz [13, 28, 36, 37], the modulus was taken to be negligibly close to the real component, and used as the principal impedance measure. As it is no longer necessary to employ a second paired recording to compensate for variable decay in an applied square wave [18], the recording time is lessened compared to the previous method.

2.2 System and experimental design considerations

The system was designed in order to be suitable for imaging fast neural activity with either epicortical or, eventually, scalp electrodes, although only epicortical or crab nerve recordings are presented here. For cortical recordings, peak changes might be expected to be about 0.1% on a standing voltage of several millivolts, i.e. of the order of 10 μV. In contrast, the principal source of noise was the EEG or ECoG for epicortical recordings. This was generally about 100× larger than the change—about 1 mV

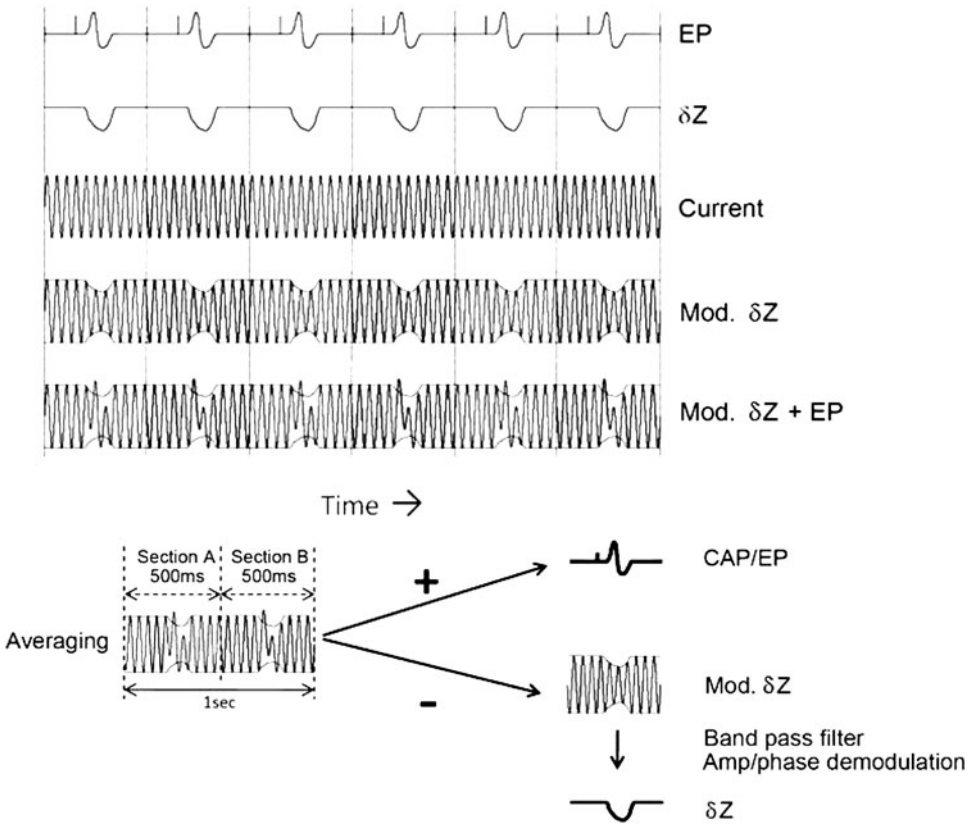

Fig. 2 Diagrammatic illustration of sine wave method. An evoked potential (or compound action potential, for nerve) (EP) is produced every 0.5 s or so. This produces a resistance change lasting for approx. 50 ms. A sine wave constant current is injected which is synchronized in phase and then in antiphase for each successive EP. The resulting sine wave voltage is modulated by the resistance change. The recorded voltage comprises the modulated sine wave and added evoked potential. The recorded signal is averaged into epochs of pairs of EPs (1 s in this example). The first and second segment of each pair are added to recover the resistance change; the resistance change is produced by subtraction and demodulation

on the cortex. As it was uncorrelated, it could be reduced by filtering and time-locked averaging to a repeated stimulus. This therefore required a high dynamic range and linearity in the recording amplifiers—we employed a recording system with 18 bit or 22 bit resolution for crab nerve or cortical studies and a linearity in both recording systems of <0.05%.

In addition, in order to derive the impedance change, it was necessary to subtract paired recordings, in which the nervous activity was two orders of magnitude larger than the voltage change related to the impedance signal in the case of crab nerve. As a result, any jitter in timing could have produced substantial artefacts. It was therefore necessary to design a system with tightly linked clocks, so as to minimise jitter and testing was undertaken with relay driven resistors to verify that the apparent impedance change was not due to jitter artefact.

A second consequence of the paired recording approach was the need to ensure that the evoked nervous activity, which was subtracted out in calculating the impedance change, was identical in paired recordings. In theory, the injected current might have distorted the waveform. This was a greater problem with the previous square wave method [18], where alternating polarities were injected into each segment of the pair to record impedance. In this case, a sine wave from 125 to 825 Hz was injected. As it was alternating, it might be expected that stimulation of nervous activity might be lessened, or, if present, be equal in both segments of the pair. However, the phase varied by 180° for each segment and this might in theory have distorted the evoked activity differently. The safe current levels to avoid this are the subject of considerable debate (reviewed in [17]). A reasonable level, based on a literature review, at which electrical stimulation will alter nervous function, is c. 1 A m^{-2} for applied currents of up to 300 Hz, which equates to $\sim$1 μA for an electrode about 1 mm^2 in area, as in this study. For the intended application, it is desirable to inject as much current as possible, as the EEG/ECoG noise is fixed whereas the impedance change will vary directly as the injected current. It was therefore essential to determine the optimal level of current which will maximise the impedance SNR while avoiding neural stimulation and so artefactual changes. In principle, it could be difficult to evaluate if any nervous stimulation was occurring during impedance recording, as any such artefactual changes would be mixed in with those resulting from the impedance change. The principle adopted in these studies, in both crab nerve and cerebral cortex, was to determine if the apparent impedance change was independent of the current level.

2.3 Instrumentation

2.3.1 Crab nerve studies

Electronic instrumentation comprised an ultra low noise programmable constant current source which could produce a sinusoidal waveform from 1 Hz to 1 kHz with an amplitude of 0.1–100 uA, the 'UCL-CS1'. This was constructed from a FPGA (EP1K50, Altera, USA), programmed as a main controller and digital waveform generator. It received commands from a PC and produced timing and control signals to the acquisition system. The sine waveform was digitally generated in a ROM which contained 2,000 samples of sine waveform data which were read by the FPGA and able to generate frequencies from 125 to 825 Hz. The DC component and high frequency clock noise were rejected by a band pass filter (10 Hz–10 kHz). There were two independent current sources to supply 0.1–10 μA or 10–100 μA. These comprised a floating Howland current source which contained digitally controlled potentiometers (DS1267-010 and DS1267-050, Dallas, USA) to equal provide equal resistance ratios. Power was supplied from batteries. The output impedance was over 1 MΩ. Voltages were recorded with a 1 channel Neurolog pre-amplifier (NL106, Digitimer, UK), filter unit (NL125, Digitimer, UK), with a gain of 50 and bandpass of DC to 10 kHz. Data were sampled at 160 kHz by a National instruments 16 bit data acquisition system set to oversample and so provide 18 bit resolution (NI USB 6259, National Instruments, USA). The system was optically isolated and controlled by a Windows PC. The current source and voltage measurement unit operated synchronously. A control signal generated from UCL-CS1 was passed to the NI data acquisition system which in turn produced a timing control signal for nerve stimulation using a driven buffer (NL510) and isolated stimulator (NL800A, Digitimer, UK) which was a battery powered and opto-coupled. All systems operated with the same clock (Fig. 3).

2.3.2 Rat cerebral cortex

An identical current source was employed, but a 32 × 8 analogue switch array was added to the front stage to permit addressing of any pair of 29 electrodes in the electrode array. The output impedance of current source was over 1 MΩ. The same isolated stimulator (NL800A, Digitimer, UK) was employed to produce somatosensory stimulation. Recording was performed with a 32 channel EEG acquisition system (SD32R, Micromed, Italy) which was modified to provide a dynamic range of 102.4 mV. Sampling was with 22 bit A/D at 2 kHz per channel and hardware filters of 0.15–570 Hz (Fig. 3).

2.4 Experimental preparations

2.4.1 Walking leg nerve of the edible crab, Cancer pagurus

Nerves were extracted from the walking leg of the edible crab, *Cancer pagurus* [25] and placed within a square groove 1.5 mm wide by 1.5 mm deep in a block of Perspex (20 × 4 cm). Electrodes comprised platinum or chloride silver foil (1.5 mm wide) placed in perpendicular grooves, 1.5 mm wide by 3 mm deep, except for the ground electrode which was 2 mm wide. Since silver is toxic to nerves, all electrodes were made of platinum apart from the measurement electrodes, R1 and R2, which were silver/silver chloride in order to yield low noise from the electrode–electrolyte interface. In order to avoid direct contact of the nerves with the silver, the central 1 cm or so of the electrode grooves near the nerve were filled with agar equilibrated with Crab Ringer's solution. The entire array was kept at a temperature of 4°C by bathing in ice water.

Nine electrodes were used and comprised two for stimulation of the action potential (S1, S2), a ground electrode (G), four for injection of the square wave current for resistance measurements (D1–D4—two were selected at a defined spacing for any one recording) and two for

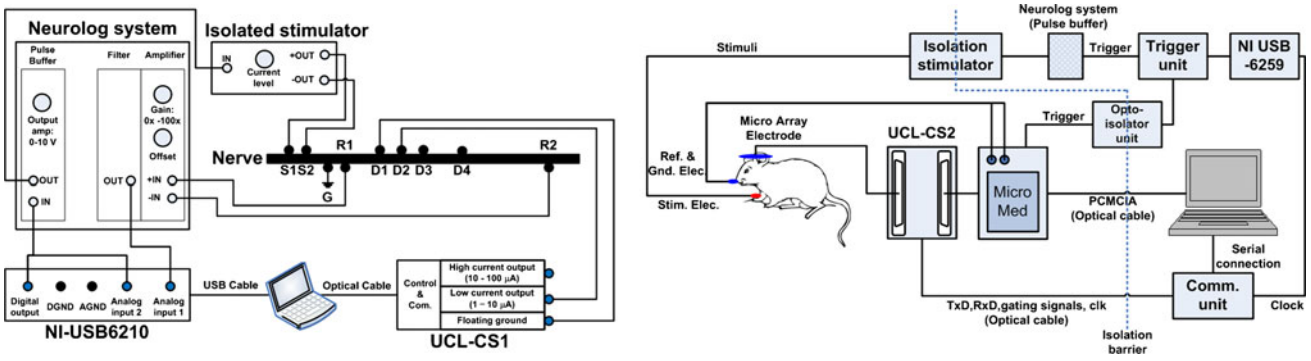

Fig. 3 *Left* Instrumentation for crab nerve recordings. *Right* Instrumentation for recordings on rat cerebral cortex

recording the resulting potentials (R1, R2). The spacing between electrode pairs S1–S2, S2–G, G–R1 and D1–D2 was 2 mm; R1–D1 was 3 mm; D1–D3 was 4 mm; D1–D4 was 8 mm and D4–R2 was 100 mm (Fig. 3).

These spacing values were between the outer edges of the electrodes. Once placed within the longitudinal groove, the nerve was immersed in crab Ringer's solution made of 525 mM/l NaCl, 13.3 mM/l KCl, 12.4 mM/l $CaCl_2$, 24.8 mM/l $MgCl_2$ and 5 mM/l dextrose. The nerve was blotted using filter paper at the start of each 1 min recording and then irrigated again as soon as it was completed. This preparation was used previously for similar square wave impedance studies [18].

Compound action potentials were produced at 2 stimuli/s by uni-polar pulses of approximately 3 mA and 500 us duration through electrodes S1–S2 to produce supramaximal stimulation. 225 recordings were made in 15 different nerves at frequencies of 125,175, 475 and 825 Hz and currents of 0.5, 1, 2, 5 and 10 μA for drive electrode spacing of 2 mm, and with spacing of 2, 4 and 8 mm with applied current of 5 μA and all frequencies. In three nerves, recordings were also made with a current phase shift of 90° at all frequencies, at 175 Hz for drive electrode spacing of 2 mm and current of 5 and 10 μA. The frequencies were chosen as multiples of 25 Hz to be far from any harmonics of 50 Hz mains noise which were filtered out during the analysis.

2.4.2 *Resistor and agar phantom validation*

The UCL-CS1 was tested by recording from a 1.5 kΩ resistor to which the drive and record circuits were connected in a four terminal mode with a parallel 430 Ω and 22 nF and series 200 Ω resistor to simulate electrode impedance. A reed relay was used to switch in a resistor of 330 kΩ in parallel with the 1.5 kΩ for periods of 20 ms to produce a transient resistance decrease of 0.38%. Noise was examined with the groove of the crab nerve array filled with agar equilibrated with crab Ringer's solution. Recording in both cases was with a current of 1 μA at 125 Hz with averaging over 1 min.

2.4.3 *Somatosensory evoked responses in the cerebral cortex of the rat, recorded with epidural electrodes*

Female Sprague-Dawley adult rats were induced and then anaesthetized with halothane (0.5–1.5% maintenance) in a mixture of 50/50% nitrous oxide/oxygen. A tracheostomy was performed and they were paralysed with pancuronium bromide and ventilated. The femoral artery and vein were cannulated and normal saline was infused at 1 ml/h. ECG, heart rate, end-tidal CO_2, blood pressure were continuously monitored and paralysis was allowed to lift every 90 min or so in order to ensure surgical anaesthesia was maintained. Blood gases were analysed every 90 min and acid–base status was maintained with normal limits by infusion of sodium bicarbonate. All work was conducted under UK Home Office regulations.

A craniotomy was performed to expose one cerebral hemisphere widely. The dura was resected and recordings were made with a custom designed electrode array, 8 × 8 mm placed on exposed cortex. This was constructed of platinum foil on a silicone rubber backing which had been laser cut to provide 29 circular electrodes, 0.6 mm in diameter, hexagonally arranged with a centre-to-centre distance of 1.2 mm. The electrodes were platinized to reduce contact impedance and noise from the electrode–electrolyte interface [40] (Fig. 7).

Somatosensory evoked responses were produced by stimulation of the contralateral forepaw with pulses 100 μs in duration and 5–10 mA at 2 Hz. Cortical evoked potentials were first recorded by averaging 128 responses. The electrode array was repositioned if needed so that the maximum response was near the centre of the array. Impedance was then recorded by averaging for 5 min with evoked response stimulation at 2 Hz. Current was injected from adjacent electrodes located where the EP was maximal in the preliminary EP recordings and voltages were recorded from the remaining 27 channels. For the effect of frequency, 51 recordings were taken from six rats, all with current of 5 μA. Frequencies tested were 125, 225, 325, 625 and 1225 Hz. For the effect of current, 64 recordings were taken from 11 rats, all with frequency of 225 Hz. Currents tested were 2, 5, 10, 20, 50 and 100 μA.

2.5 Method for calculation of the impedance change

Compound action or evoked potentials were produced every 0.5 s. A constant current sine wave was applied which was in phase for the first 500 ms segment and antiphase for the next. 60 or 300 such paired epochs comprised one recording for crab or rat, respectively, and were averaged. The two 500 ms phases were summed to produce the compound or evoked potentials. The impedance modulus was produced by subtracting the first and second segment. The modulated carrier was then demodulated by: (1) the signal from the subtracted segments was band pass filtered with a bandwidth of 250 Hz to eliminate most of the residual noise at the EEG band (<100 Hz) left after the averaging as well as high frequency instrumentation noise. (2) Then, demodulation was performed by calculating the absolute values and phases on an analytic version of the signal, created using the Hilbert transform. The modulus of the resulting change was taken to be the real component.

2.6 Data analysis

For the crab case, the entire dataset of 225 recordings was inserted into a four way analysis of variance to evaluate the effect of frequency, current, spacing and phase of applied current. Analysis indicated an effect of the highest current applied, 10 μA. These recordings were excluded for further analysis, leaving 209 recordings. For rat cortical recordings, the effect of current and frequency were analysed with one way Anova with repeated measures. Results are presented as mean ± 1SE.

3 Results

3.1 Validation of experimental setup

With the switched resistor network, a resistance change of −0.38% was recorded as 0.36% in peak amplitude. The effects of filters in the recording circuit were examined with computer simulation. A square wave voltage change of −0.12% lasting 20 ms was recorded with a peak change of −0.10% after filtering. With the crab nerve recording block filled with agar, the noise was less than 0.95 μV_{pp}. With injection of 125 Hz, 1 μA current into the agar, with R1–R2 spacing of 2 mm, the noise was 0.4 μV_{pp}, equivalent to 0.05%.

3.2 Crab nerve

There were consistent significant decreases in impedance in all nerves tested with a similar time course to the compound action potential (225 recordings in 15 nerves) (Fig. 4). δZ did not vary significantly with applied current of 0.5–5 μA ($P = 0.25$) but decreased at all frequencies with 10 μA (Fig. 5, $P < 0.001$). For example, with applied current of 5 μA and R1–R2 spacing of 2 mm, δZ was −0.25 ± 0.02, −0.16 ± 0.01, −0.09 ± 0.01 and −0.06 ± 0.003% for applied frequencies of 125, 175, 475 and 825 Hz, respectively. δZ also decreased with increasing spacing of the drive electrodes for all four applied frequencies and applied current of 5 μA (Fig. 6, $P = 0.18$). There was no significant change in δZ with applied phase of 0 or 90° ($P = 0.97$). Both the decrease in δZ with frequency and recording electrode spacing were in concert with biophysical modelling [32].

3.3 Cortical recordings during somatosensory evoked responses in the anaesthetised rat

Evoked potentials of 150–800 μV were recorded which lasted for up to 200 ms with an N12 peak. Reproducible resistance and phase changes could be observed with a distribution around the electrodes used for current injection, with an appropriate pattern for the greatest current density. These could be observed reliably in approximately one third of electrodes and had a time course which corresponded to the evoked potential, peaking at about 12 ms. The signal to noise increased with applied current. With an applied current of 50 μA, the SNR was approximately 50 in many channels (Fig. 7). The peak changes were −0.074 ± 0.01, −0.070 ± 0.006, −0.027 ± 0.005, −0.022 ± 0.003 and −0.01 ± 0.01% for current applied at 125, 225, 325, 625 and 1225 Hz ($n = 51$ in six rats), respectively, (Fig. 8). The size of the changes significantly decreased with increased frequency ($P = 0.00001$). The changes were constant with applied current up to 50 μA ($n = 64$, 11 rats, 225 Hz, $P = 0.68$) but decreased, although not significantly, with current injected at 100 μA ($P = 0.14$) (Fig. 8).

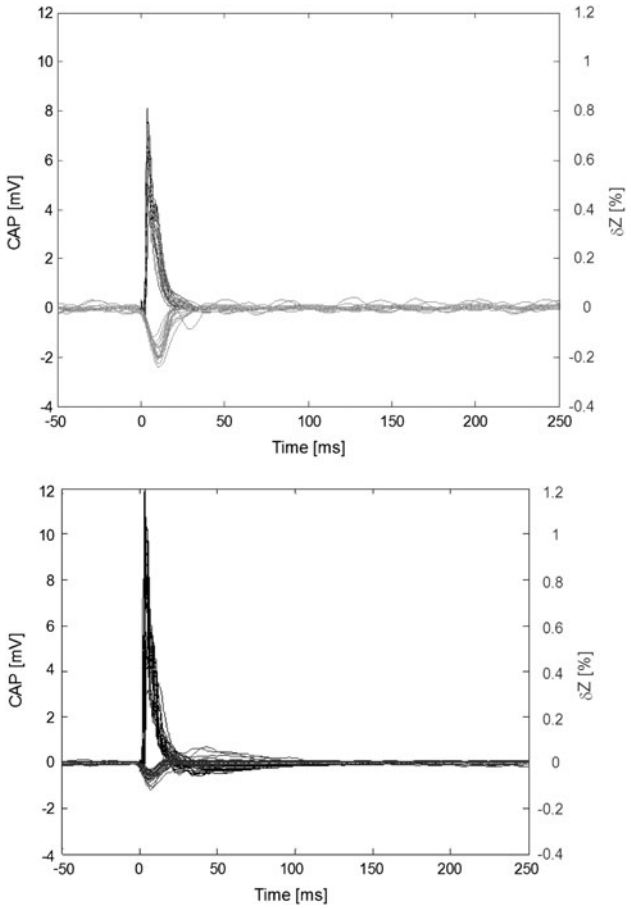

Fig. 4 Examples of compound action potential (positive, *black*) and associated resistance change (δZ, negative, *grey*). *Top*: 125 Hz, $n = 16$ in 1 nerve. Peak δZ was −0.18 ± 0.002%, $\delta\Phi$ 0.10 ± 0.002° and CAP 6.2 ± 0.07 mV. *Bottom*: 825 Hz, $n = 30$ in 1 nerve. Peak δZ was −0.06 ± 0.0007%, $\delta\Phi$ 0.18 ± 0.0007° and CAP 8.4 ± 0.08 mV (2 mm R1-R2 spacing, 2 μA, zero phase in both cases)

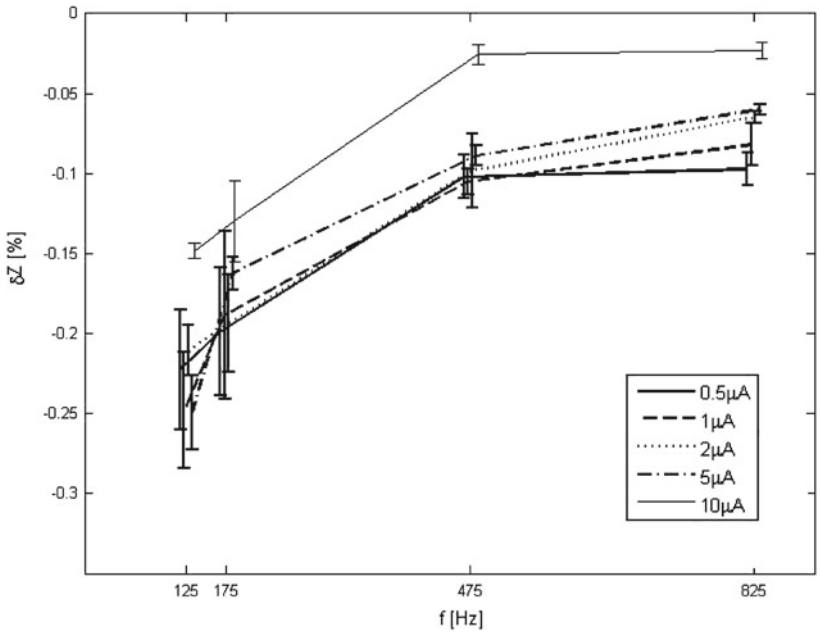

Fig. 5 Impedance changes (δZ) in crab nerve during the compound action potential. *Top* Changes with frequency for different applied currents (mean ± 1 SE, recordings (nerves)). *Bottom* Comparison of experimentally recorded δZ over frequency (5 μA, D1–D2 2 mm) measured in this study and at 1 Hz in [18] with predictions from biophysical modelling [32] normalised to the measured change at 1 Hz

I [μA]	0.5	1	2	5	10
Hz					
125	-0.22±0.04/4(2)	-0.25±0.04/4(2)	-0.21±0.02/20(3)	-0.25±0.02/16(6)	-0.148±0.005/4(1)
175	-0.20±0.04/4(2)	-0.19±0.05/4(2)	-0.19±0.03/4(2)	-0.16±0.01/16(6)	-0.13±0.03/4(1)
475	-0.10±0.01/4(2)	-0.11±0.01/4(2)	-0.10±0.02/4(2)	-0.09±0.01/17(6)	-0.03±0.01/4(1)
825	-0.10±0.01/4(2)	-0.08±0.01/4(2)	-0.064±0.004/34(3)	-0.060±0.003/18(6)	-0.023±0.005/4(1)

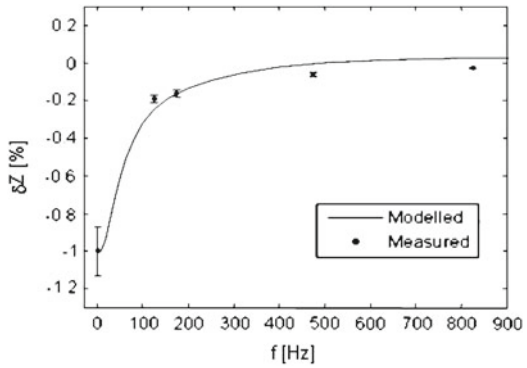

4 Discussion

We describe a novel method for recording impedance changes at low sinusoidal frequencies which has the potential to provide a foundation for the advance of tomographic imaging of fast neural activity in the brain with EIT. The principal concerns were whether the applied current and its phase might itself interfere with nervous function, whether there might be recording artefacts related to the necessary method of subtraction, and whether it could, in the event, yield cortical signals with a satisfactory SNR. The criteria for believing that the changes observed in this study were physiological and genuine were that they agreed with the modelling and also were independent of the applied current. These appear to have been met: in crab nerve, reproducible changes of 0.25% at 125 Hz and 5 μA were observed which decreased to 0.06% at 825 Hz. They were constant with applied current up to 5 μA and with phase and their frequency response and variation with recording electrode spacing were as anticipated from modelling. In comparison, in a previous study, resistance changes under similar conditions with current injection at 1 Hz with a square wave were larger—1.0 ± 0.13% [18], which also fits the model. The crab nerve studies permitted validation and refinement of the method, although there is no interference from spontaneous activity, which was the principal constraint on imaging in our previous study with scalp electrodes in humans. In rat cortical recordings, where there were large ECoG changes which might potentially have obscured the impedance change, it was

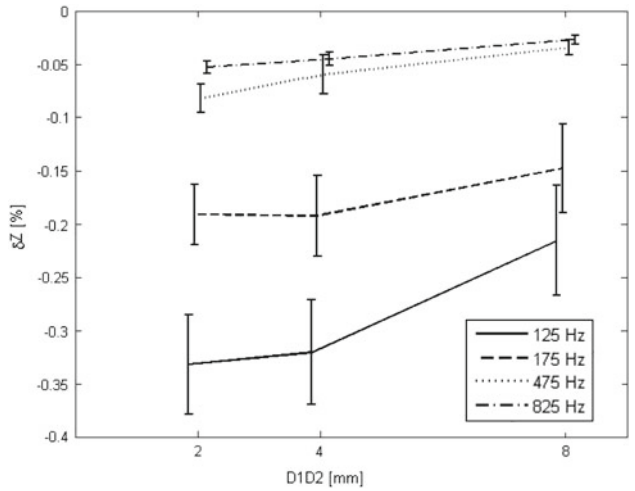

Spacing [mm]	2	4	8
Frequency [Hz]			
125	-0.33±0.05	-0.32±0.05	-0.22±0.05
175	-0.19±0.03	-0.19±0.04	-0.15±0.04
475	-0.08±0.01	-0.06±0.02	-0.03±0.01
825	-0.05±0.01	-0.05±0.01	-0.027±0.004

Fig. 6 Impedance changes (δZ) in crab nerve during the compound action potential. Effect of electrode spacing between drive electrodes, D1 and D2 on δZ [%] for each frequency (mean ± 1 SE, recordings (nerves); all $n = 4$ in 2 nerves except 2 mm/475&875 Hz, $n = 5$)

possible to observe reliable impedance changes, for the first time, which again matched modelling and were physiologically plausible. The optimum settings were applied current of 225 Hz and 50 μA which yielded peak changes with an SNR of 50.

In selecting carrier frequencies for recording the impedance signal, the main consideration was to maximise the SNR. This was achieved by a balance between maximising the magnitude of the impedance change ('the signal') at low frequencies and minimising the background EEG signal ('the noise') at high frequencies as well as selecting a pass band which excluded most of the EEG band. A secondary technical consideration was to use a carrier frequency in between any pair of mains 50 Hz harmonics to best enable their cancellation. Several frequencies in the range 125–825 Hz were assessed. In the event, the optimal frequency was 225 Hz. An optimal bandwidth was selected as ±125 Hz, as this enabled satisfactory capture of the EP related impedance change while excluding most of the EEG noise. Unfortunately, this combination of carrier frequency and bandwidth introduced a possible artefact due to aliasing. In principle, a carrier frequency must exceed half the bandwidth of the modulated signal to avoid aliasing (Fc > BW/2) as any

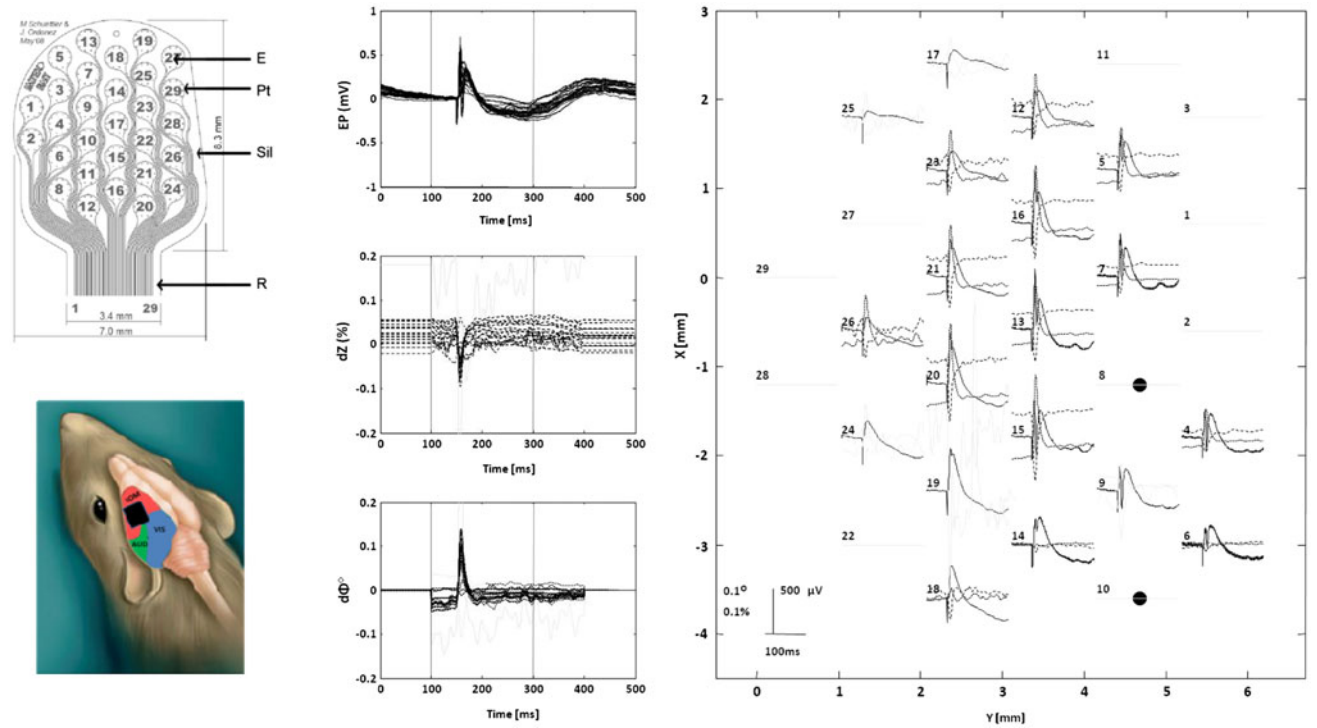

Fig. 7 Example of recording from rat cerebral cortex during forepaw somatosensory stimulation. *Upper left*: Design of electrode array; *E* electrode site, *Pt* platinum, *Sil* silicone rubber substrate, *R* ribbon cable and diagrammatic illustration of its position on exposed rat cerebral cortex. *Middle*: Superimposed from all channels: evoked potentials (EP, *solid*), impedance change (δZ, *dashed*), phase change ($\delta\Phi$, *dotted*). *Right*: EP, δZ and $\delta\Phi$ displayed topographically over the cortex. Current, 225 Hz, 50 μA, was applied through electrodes 8 and 10 (*filled circles*). Peak evoked activity (EP, *solid line*) may be seen from electrode 13 (centre of display). Electrodes with >0.05% noise are *greyed* out. Resistance changes of up to 0.2%, SNR ~50, may be seen with a similar distribution of amplitude to the evoked potentials

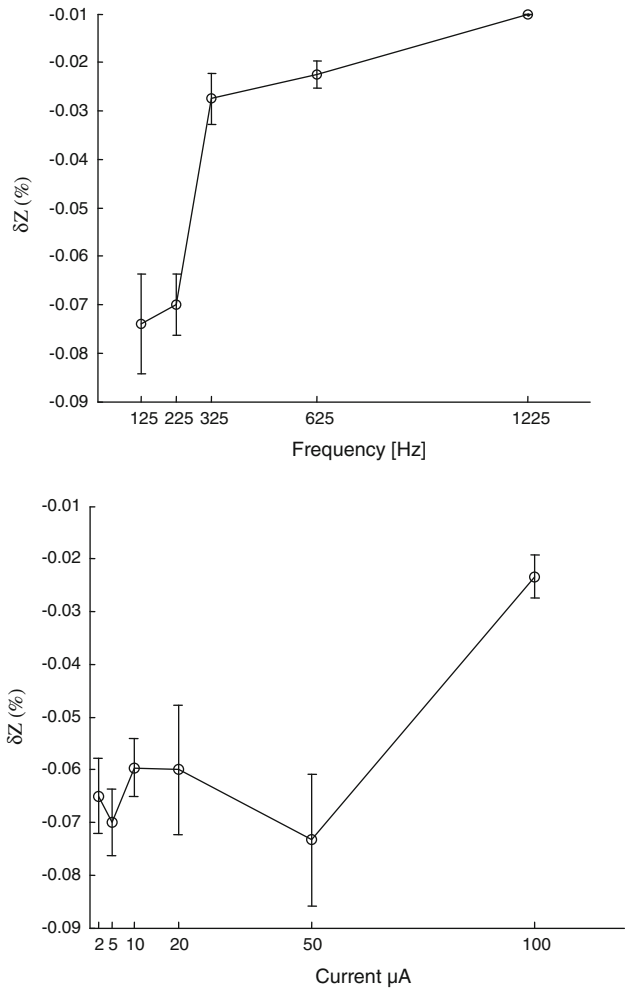

Fig. 8 Change in δZ during evoked responses in rat cortex with varying frequency (*upper*) and current (*lower*)

modulated frequency components above the carrier frequency will reach the negative frequencies domain and will fold back into the positive frequency domain. As the actual impedance change might have frequency components above 225 Hz—especially a compound action potential in crab, this could in theory have introduced an artefact during any demodulation procedure. To address this potential problem, we have modelled a fast impedance change with frequency content similar to the CAPs of the crab. This indicated that any such aliasing artefact altered the resulting demodulated impedance changes by <10% of their original vales. Therefore, this indicated that this source of artefact was negligible. For rat recordings, this artefact is even lower as the highest frequency components of EEG and EPs were lower than those for compound action potentials.

The temporal resolution of the recordings was determined by the electronic hardware employed. For the crab recordings, a single channel amplifier and fast A/D converter, sampling at 160 kHz was used, so that recording with current applied at up to 825 Hz could be accomplished with a time constant of 1 ms. For rat recording, a commercial EEG amplifier was used, with which the maximum sampling rate was 2 kHz per channel and a hardware anti-aliasing filter of 570 Hz limited the recording bandwidth. As it was desirable to restrict the bandwidth to avoid the EEG in the band of 1–100 Hz, we set the bandwidth to ±125 Hz in order to enable recording at 225 Hz. This rendered the time constant for rat cortical recordings to be 8 ms. This permitted demonstration of proof of principle but a lower constant of perhaps 1 ms would be desirable in the future. For future studies, electronic hardware with a higher sampling rate and anti-aliasing filter could be used. With this, the possibility of using a higher carrier frequency could be explored, which could permit a higher bandwidth and temporal resolution, although this might be at the expense of SNR.

An important consideration was the choice of applied current. In order to improve SNR, it was desirable to inject as much as possible, but the integrity of the method depended on subtraction of the evoked neural response, so it was essential that the applied measuring current did not alter the response and produce artefactual apparent impedance changes. For the crab nerve, the maximal current that could be applied, 5 μA, is relatively close to the threshold mentioned above in the introduction, of about 1 μA. For the case of the rat cortex, we observed that the SNR of recordings with 5 μA current injection was only about 5. Although it appeared to exceed the above limit, we assessed higher applied currents. In the event, both the evoked potentials and impedance responses appeared to be unaffected up to 50 μA, which was unexpected. The explanation is not entirely clear. It seems probable that the current limit depends critically on current dispersion from the electrode. Whereas it may be possible that neurones very close to the injecting electrodes are indeed affected, this rapidly falls off, so that neural activity in the region of interest, several mm away, is not.

Electrical impedance tomography (EIT) of fast neural activity appears to offer unique advantages as currently there is no other method which has the potential to offer imaging over the entire brain. Possible macroscopic scale neuroimaging methods include source modelling of the EEG [1] and MEG [21], their multimodality fusion with MRI [9], direct mapping with MRI [20, 35] and diffuse optical tomography [15]. At a smaller scale, two-dimensional mapping of fast cortical activity may be achieved with voltage sensitive dyes [7] or activity in individual neuronal processes may be imaged over a volume up to 100 μm along each edge with two-photon imaging of calcium transients using a fluorescent dye [27]. There has also been recent interest in the use of MR-EIT for imaging fast

neural activity, in which MRI is used to image conductivity changes recorded with simultaneously applied current [39]. However, to our knowledge, there is presently no method which could permit imaging of fast neuronal depolarization through the brain with a resolution of a few mm and ms: inverse source modelling of the EEG and MEG do not have a unique inverse solution, neuronal current MRI presently lacks sufficient sensitivity, it is unclear if MR-EIT would have sufficient sensitivity if medically safe currents are applied to the scalp, voltage sensitive dye and imaging is restricted to the cortical surface or penetration of visible light, and two photon calcium imaging is restricted to small volumes of cortex a few hundred μm across and with limited sampling within these.

An advantage of this potential application of EIT over inverse source modelling of the EEG or MEG is that this mechanism effectively rectifies the recording of ionic channel opening—resistance across the membrane can only fall. In this way, impedance falls irrespective of whether the neurotransmitter giving rise to the change is excitatory or inhibitory. Neuroelectric or neuromagnetic signals cancel out when measured from a distance unless the neuronal processes are spatially aligned, as in the dendritic tree of the pyramidal cells. The rectified resistance change could capture activity in the entire depolarized tissue, regardless of the spatial arrangement, so the opportunity to record the changes from a distance are much greater.

In addition, the inverse solution for EIT is in principle unique for the idealised case where there is complete and noise-free knowledge of all boundary potentials with all possible current injections and sufficient 'smoothness' of the unknown conductivity profile [6, 29], unlike that for inverse source modelling where a variety of constraints of indeterminate validity must be employed to give a solution [2]. However, some constraints are also needed in EIT solutions in practice, where the inverse solution is ill-posed and there are discrete measurements and instrumentation errors. Nevertheless, in experimental studies, somewhat blurred but consistently reliable images may be obtained for test objects in anatomically realistic head-shaped saline filled tanks containing a human skull [11].

There are several reports in the literature of attempts to record impedance changes during evoked activity in neural tissue. The frequency of applied current is a critical factor as the modelling above indicates that, in theory, the magnitude of changes expected falls off rapidly with increasing frequency over about 100 Hz. This is because, above this frequency, current starts to pass into the intracellular space at rest by crossing the capacitance of cell membranes; there is therefore a much smaller change when ion channels open during activity and current starts to pass into the intracellular compartment by this resistive route. Findings vary from resistance decreases of 3.1% ± 0.8 (SE) during direct cortical stimulation in the cat, using a four electrode system and square wave pulses 0.3–0.7 ms in duration [12] to 0.003% in the cortex [30, 31], and of 0.03% in subcortical nuclei [14] during visual and auditory evoked responses in the cat at 10 kHz. At 50 kHz, no changes larger than background noise of about 0.01% were observed during direct electrical stimulation of the cerebral cortex in rats [26] or during somatosensory, auditory and visual evoked responses in humans [23]. These are broadly in agreement with the current findings and modelling.

Overall, these findings were most encouraging to the view that it may be possible now to proceed to tomographic imaging of fast neural activity. The work has permitted optimisation of technical aspects of the method and illuminated the need for precise timing to avoid jitter artefact. It also allowed assessment of optimal recording parameters, which were use of applied current of 225 Hz and 50 μA for recording during evoked activity in rat cerebral cortex. The time required to generate data appears to be practicable—with 50 μA applied current, high quality data may be collected in 1 min. Tomographic imaging requires collection of data with current injection through perhaps 30 different electrode pairs. This suggests a total recording time of about 30 min, which is feasible for the repeatable paradigm of cortical evoked activity. The ultimate goal is to apply this method to imaging fast neural activity with scalp electrodes. In principle, a similar SNR might be expected, as both the signal and principal noise source, the EEG, might be expected to be reduced in a similar fashion by the voltage dividers of the skull and extracerebral layers. However, instrumentation noise may come to limit SNR with the overall smaller signals and there will undoubtedly be several technical challenges, such as the need to inject similar current densities through the skull and spatial low pass filtering effects of the skull. However, these latter have already been overcome to a considerable extent in previous studies [17, 19] so this appears to be at least a plausible prospect. Work in progress is to validate the new method with epicortical imaging in a rat model, with reduction in total acquisition time, and then proceed to human studies.

Acknowledgments The National Institutes of Health (NIH), US under Grant 5R01EB006597-03 from the National Institute of Biomedical Imaging and Bioengineering (NIBIB) and the National Eye Institute (NEI).

References

1. Baillet S, Riera JJ, Marin G, Mangin JF, Aubert J, Garnero L (2001) Evaluation of inverse methods and head models for EEG source localization using a human skull phantom. Phys Med Biol 46:77–96

2. Bleistein N, Cohen KJ (1977) Nonuniqueness in the inverse source problem in acoustics and electromagnetics. J Math Phys 18:194–201
3. Boone KG (1995) The possible use of applied potential tomography for imaging action potentials in the brain. PhD thesis, University College London, London, UK
4. Boone KG, Holder DS (1995) Design considerations and performance of a prototype system for imaging neuronal depolarization in the brain using 'direct current' electrical resistance tomography. Physiol Meas 16:A87–A98
5. Brown BH, Seagar AD (1987) The Sheffield data collection system. Clin Phys Physiol Meas 8(Suppl A):91–97
6. Calder′on AP (1980) On an inverse boundary value problem. In: Meyer WH, Raupp MA (eds) Seminar on numerical analysis and its applications to continuum physics. Brazilian Mathematical Society, Rio de Janeiro, pp 65–73
7. Chemla S, Chavane F (2010) Voltage-sensitive dye imaging: technique review and models. J Physiol Paris 104:40–50
8. Cole SK, Curtis HJ (1939) Electrical Impedance of the squid giant axon during activity. J Gen Physiol 22:649–670
9. Dale AM, Halgren E (2001) Spatiotemporal mapping of brain activity by integration of multiple imaging modalities. Curr Opin Neurobiol 11:202–208
10. Fabrizi L, Sparkes M, Horesh L, Perez-Juste Abascal JF, McEwan A, Bayford RH, Elwes R, Binnie CD, Holder DS (2006) Factors limiting the application of electrical impedance tomography for identification of regional conductivity changes using scalp electrodes during epileptic seizures in humans. Physiol Meas 27:S163–S174
11. Fabrizi L, McEwan A, Oh T, Woo EJ, Holder DS (2009) A comparison of two EIT systems suitable for imaging impedance changes in epilepsy. Physiol Meas 30:S103–S120
12. Freygang WH, Landau WM (1955) Some relations between resistivity and electrical activity in the cerebral cortex of the cat. J Cell Physiol 45:377–392
13. Gabriel S, Lau RW, Gabriel C (1996) The dielectric properties of biological tissues: II. Measurements in the frequency range 10 Hz to 20 GHz. Phys Med Biol 41:2251–2269
14. Galambos R, Velluti R (1968) Evoked resistance shifts in unanaesthetized cats. Exp Neurol 22:243–252
15. Gibson A, Dehghani H (2009) Diffuse optical imaging. Philos Trans A 367:3055–3072
16. Gilad O, Holder DS (2009) Impedance changes recorded with scalp electrodes during visual evoked responses: implications for electrical impedance tomography of fast neural activity. Neuroimage 47:514–522
17. Gilad O, Horesh L, Holder DS (2007) Design of electrodes and current limits for low frequency electrical impedance tomography of the brain. Med Biol Eng Comput 7:621–633
18. Gilad O, Ghosh A, Oh D, Holder DS (2009) A method for recording resistance changes non-invasively during neuronal depolarization with a view to imaging brain activity with electrical impedance tomography. J Neurosci Methods 180: 87–96
19. Gilad O, Horesh L, Holder DS (2009) A modelling study to inform specification and optimal electrode placement for imaging of neuronal depolarization during visual evoked responses by electrical and magnetic detection impedance tomography. Physiol Meas 30:S201–S224
20. Hagberg GE, Bianciardi M, Maraviglia B (2006) Challenges for detection of neuronal currents by MRI. Magn Reson Imaging 24:483–493
21. Hamalainen MS, Hari R, Ilmoniemi RJ, Knuutila J, Lounasmaa OV (1993) Magnetoencephalography-theory, instrumentation, and applications to noninvasive studies of the working human brain. Rev Mod Phys 65:413–497
22. Holder DS (1987) Feasibility of developing a method of imaging neuronal activity in the human brain: a theoretical review. Med Biol Eng Comput 25:2–11
23. Holder DS (1989) Impedance changes during evoked nervous activity in human subjects: implications for the application of applied potential tomography (APT) to imaging neuronal discharge. Clin Phys Physiol Meas 10:267–274
24. Holder DS (1992) Detection of cerebral ischaemia in the anaesthetised rat by impedance measurement with scalp electrodes: implications for non-invasive imaging of stroke by electrical impedance tomography. Clin Phys Physiol Meas 13:63–75
25. Holder DS (1992) Impedance changes during the compound nerve action potential: implications for impedance imaging of neuronal depolarisation in the brain. Med Biol Eng Comput 30:140–146
26. Holder DS, Gardner-Medwin AR (1988) Some possible neurological applications of applied potential tomography. Clin Phys Physiol Meas 9(Suppl A):111–119
27. Homma R, Baker BJ, Jin L, Garaschuk O, Konnerth A, Cohen LB, Zecevic D (2009) Wide-field and two-photon imaging of brain activity with voltage- and calcium-sensitive dyes. Philos Trans R Soc Lond B 364:2453–2467
28. Horesh L, Gilad O, Romsauerova A, McEwan A, Arridge SR, Holder DS (2005) Stroke type differentiation by multi-frequency electrical impedance tomography—a feasibility study. Proc 3rd Eur Med Biol Eng Conf: 1252–1256
29. Isaacson D, Isaacson EL (1989) Comment on Calderon's paper: "On an Inverse Boundary Value Problem". Math Comput 52:553–559
30. Klivington KA, Galambos R (1967) Resistance shifts accompanying the evoked cortical response in the cat. Science 157:211–213
31. Klivington KA, Galambos R (1968) Rapid resistance shifts in cat cortex during click-evoked responses. J Neurophysiol 31:565–573
32. Liston AD (2004) Models and image reconstruction in electrical impedance tomography of human brain function. PhD thesis, Middlesex University, London, UK
33. McEwan A, Romsauerova A, Yerworth R, Horesh L, Bayford R, Holder D (2006) Design and calibration of a compact multifrequency EIT system for acute stroke imaging. Physiol Meas 27:S199–S210
34. Metherall P, Barber DC, Smallwood RH, Brown BH (1996) Three-dimensional electrical impedance tomography. Nature 380:509–512
35. Parkes LM, de Lange FP, Fries P, Toni I, Norris DG (2007) Inability to directly detect magnetic field changes associated with neuronal activity. Magn Reson Med 57:411–416
36. Ranck JB Jr (1963) Analysis of specific impedance of rabbit cerebral cortex. Exp Neurol 7:153–174
37. Ranck JB Jr (1966) Electrical impedance in the subicular area of rats during paradoxical sleep. Exp Neurol 16:416–437
38. Romsauerova A, McEwan A, Horesh L, Yerworth R, Bayford RH, Holder DS (2006) Multi-frequency electrical impedance tomography (EIT) of the adult human head: initial findings in brain tumours, arteriovenous malformations and chronic stroke, development of an analysis method and calibration. Physiol Meas 27:S147–S161
39. Sadleir RJ, Grant SC, Woo EJ (2010) Can high-field MREIT be used to directly detect neural activity? Theoretical considerations. Neuroimage 52:205–216
40. Schuettler M, Ordonez JS, Henle C, Oh D, Gilad O, Holder DS (2008) A flexible 29 channel epicortical electrode array. In: 13th annual conference of the international FES society, Freiburg, Germany
41. Tidswell AT, Gibson A, Bayford RH, Holder DS (2001) Three-dimensional electrical impedance tomography of human brain activity. NeuroImage 13:283–294